Pyromellitic dianhydride crosslinked cyclodextrin nanosponges for curcumin controlled release; formulation, physicochemical characterization and cytotoxicity investigations

(Article begins on next page)

07 May 2024

Pyromellitic dianhydride crosslinked cyclodextrin nanosponges for curcumin controlled release; formulation, physicochemical characterization and cytotoxicity investigations

Rafati Nesa[1], Zarrabi Ali[1,2*], Caldera Fabrizio[3], Trotta Francesco[3], Ghias Narges[4].

[1] Department of Biotechnology, Faculty of Advanced Sciences & Technologies, University of Isfahan, Isfahan, Iran.

[2] Sabanci University Nanotechnology Research and Application Center (SUNUM), Tuzla, Turkey.

[3] Department of Chemistry and NIS Centre, University of Turin, Torino, Italy.

[4] Department of Mechanical Engineering, Sharif University of Technology, Tehran, Iran.

*Corresponding author: alizarrabi@sabaniciuniv.edu

Abstract

Aim: In this study, a nanosponge structure was synthesised with capability of encapsulating curcumin as a model polyphenolic compound and one of the herbal remedies that have widely been considered due to its ability to treat cancer.

Methods: FTIR, DSC and XRD techniques were performed to confirm the formation of the inclusion complex of the nanosponge-drug.

Results: DSC and XRD patterns showed an increasing stability and a decreasing crystallinity of curcumin after formation of inclusion complex. Encapsulation efficiency was 98% (w/w) and a significant increase was observed in loading capacity (184% w/w). The results of cytotoxicity assessments demonstrated no cell toxicity on the healthy cell line, while being toxic against cancer cells. Haemolysis test was performed to evaluate the blood-compatibility characteristic of nanosponge and complex and the results showed 0.54% haemolysis in the lowest complex concentration (50µgml^{-1}) and 5.09% at the highest concentration (200µgml^{-1}).

Conclusions: Thus, the introduced system could be widely considered in cancer treatment as a drug delivery system.

Keywords: Nanosponge, curcumin, inclusion complex, solubility, anti-cancer

1. Introduction

Curcumin is a biologically active compound of the polyphenols groups that are found in turmeric, a kind of spice that comes from the rhizomes of the plant Curcuma longa Linn. Curcumin has high levels of consumption in Asian countries and has had many years of medicinal use. (Gupta et al. 2013, Mousavi et al. 2015, Nelson et al. 2017) There is great evidence that curcumin is used in trammel molecular targets. Curcumin activities, including antioxidant (Wright 2002), anti-inflammatory (Rao et al. 2013), anti-cancer (Jahed et al. 2014, Vallianou et al. 2015, Rauf et al. 2018) and neurological activities (Boyanapalli and Kong 2015). Several studies have acknowledged the role of curcumin in differentiating healthy and cancerous cells. (Ravindran et al. 2009, Hamzehzadeh et al. 2018). High consumption of curcumin is not harmful to humans and is completely safe (Lao et al. 2006, Hewlings and Kalman 2017). Curcumin consumed orally is absorbed slightly and is quickly metabolised and omitted (Lao et al. 2006, Baum et al. 2008). Due to the low bioavailability of curcumin, the potential of this substance is reduced as a therapeutic agent (Anand et al. 2007).

1

Recent evidence suggest that curcumin is an effective factor in the stoppage or treatment of some cancers, such as colon, breast, and prostate cancer (Aggarwal et al. 2003, Amanlou et al. 2019). Preclinical and clinical studies emphasise the safety of curcumin high doses, but its solubility and bioavailability are rather low, and when taken orally, it is found metabolites of curcumin in serum or plasma while curcumin is expected to be seen (Maheshwari et al. 2006, Anand et al. 2007). In addition, in anticancer therapy, the drug molecule needs to stay longer in the tumour site. Therefore, in today's research, formulation of the drug is necessary to improve bioavailability and increase dissolving capacity (Imanifard et al. 2017). The efforts of many researchers are to increase the solubility of curcumin and its slow release in place of action. One approach to increase the solubility of the drug and control its release is to use a nanostructure with an internal cavity that can accept the molecule as a guest in this cavity (Campos et al. 2013, Bhatia 2016). Moreover, these Nanoparticles formulation should have a small size, low cytotoxicity, variety and high loading capacity and bioavailability (Bhatia 2016).

New developments in the field of nanotechnology have attracted much attention to supramolecular structures with simple components. It is assumed that the design of nanomaterials with structural features in the region of nanoscale could have potential applications in drug delivery systems (Pochampally et al. 2017, Wang et al. 2018, Islami et al. 2018, Khorrami et al. 2018).

Cyclodextrins are biological compounds in molecular scale but with supramolecular traits (Zarrabi et al. 2011, Kurkov and Loftsson 2013). They are a class of multi-sugar spherical molecules of glucopyranose type that are obtained from the enzymatic degradation of starch sugar. It is a cluster compound of multicellular linear polymers in which glucose units are connected by a clamping strain and form $\alpha1$–4 bonds. Native cyclodextrins are three types α, β, and γ that have six, seven and eight glucopyranose units, respectively. They have conical shapes with a hydrophobic cavity (Zarrabi et al. 2014, Saokham et al. 2018). They are able to form inclusion and non-inclusion complexes with different drugs (Trotta et al. 2012, Jahed et al. 2014). Cyclodextrin-based nanosponges are nano-scale new drug delivery systems that consist of polymeric structures with various cross-linkers, arranged in a three-dimensional network. These kinds of cyclodextrins can form insoluble porous nanostructures with crystalline/amorphous, spherical shape and also have a swelling trait (Trotta 2011, Trotta et al. 2012, Tejashri et al. 2013, Allahyari et al. 2019). Polymer dimensions and polarisation depend on the amount and type of crosslinker (Trotta et al. 2012). The potential application of nanosponges in drug delivery systems is due to their versatility and biocompatibility. Nanosponges are used to increase the solubility of drugs, convert liquids to solids, eliminate unpleasant flavours and increase the release time of the drugs (Ferro et al. 2014, Pushpalatha et al. 2018, Trotta and Mele 2019). The EU Commission has recently announced the use of nanosponges as a novel drug delivery system. They can be used in the preparation of capsules, pills, pellets, suspensions, granules, topical pharmaceutical forms, solid dispersions or as new multifunctional carriers (Moya-Ortega et al. 2012, Simionato et al. 2019).

The ability to connect different ligands to the nanosponges surface makes them effective in targeting a particular position (Bose et al. 2016). After injecting into mice, it was found that they are tolerable and safe, biocompatible, and they have negligible toxicity (Shende et al. 2015). Cyclodextrin-based nanosponges have the ability to form inclusion and non-inclusion complexes with different types of lipophilic and hydrophilic molecules (Moya-Ortega et al. 2012, Deshmukh and Shende 2018). By modifying and manipulating the structure, the release of trapped molecules in these networks can be modified so that the release is either faster or slower (Lembo et al. 2018). In fact, apart from the dissolution phase, the drugs are molecularly scattered in the nanosponges, and in the next step, they are released. The consequence is to increase the apparent solubility of the drug (Moya-Ortega et al. 2012). The utilisation of the nanosponges is very important for designing a sustainable drug delivery system, improving the solubility of drugs that have low solubility in water, and protecting degradable molecules (Vishwakarma et al. 2014, Sherje et al. 2017). There

are extensive researches on Cyclodextrin-based nanosponges and their development to design drug delivery systems for insoluble drugs (Trotta et al. 2012, Rezaei et al. 2019).

The aim of this research was to enhance the loading capacity of synthesised nanosponges using pyromellitic dianhydride (PMDA) as the cross-linking agent. Nanosponge preparation physiochemical characterisation, drug loading and release were conducted throughout the research. Moreover, the cytotoxicity studies were implemented against cancer cells.

2. Materials and methods

2.1. Materials

Curcumin and PMDA were purchased from Sigma–Aldrich (Germany). β-cyclodextrin (β-CD) was obtained as a gift from Roquette (Italy). All other chemicals and reagents were of analytical grade. Milli-Q water (Millipore) was used throughout the studies.

2.2. Methods

2.2.1. Synthesis of β-cyclodextrin nanosponges

The NS were obtained using the synthetic procedure reported in the Italian patent (Trotta et al. 2004). Briefly, to construct nanosponge, beta-cyclodextrin and pyromellitic anhydride as the crosslinker was used. First, beta-cyclodextrin and pyromellitic dianhydride in molar ratio (1:4) were dissolved in dimethyl sulfoxide and then triethylamine was added to the aqueous solution allowing to react at room temperature. After 24 h, the gel was powdered in a mortar. The powder was then washed using Ethanol and finally was washed with Acetone and was dried by freeze dryer. Different ratios of β-CD and crosslinker improve encapsulation efficiency and modify the release profile. The effect of different ratios of B-CD and the crosslinker on the encapsulation efficiency and the release profile were investigated.

2.2.2. Preparation of curcumin-loaded NS (CRC-NS)

CRC-NSs were prepared by freeze-drying technique as previously reported (Ansari et al. 2011). Briefly accurately weighed quantities of NS were suspended in 50 ml of distilled water on a magnetic stirrer. Then, excess amount of curcumin dissolved in ethanol was added and the mixture was sonicated for 20 min and was kept for 24 h under stirring. The suspensions were then centrifuged at 3000 rpm for 15 min to separate the uncomplexed drug as a residue below the colloidal supernatant. The supernatant was then lyophilised using VaCo5, Zirbus (Germany) lyophilizer at −40°C temperature and operating pressure below 0.1 mbar to obtain drug-loaded NS formulations. The dried powder was sieved through #60 sieve and stored in a desiccator.

2.2.3. ATR-FTIR analysis investigations

Fourier Transform Infra-red (FTIR) spectra was recorded in the spectral range of 650–4000 cm^{-1} using a Perkin–Elmer Spectrum 100 instrument in the attenuated total reflectance (ATR) mode with a diamond crystal using 8 scans per spectrum and a resolution of 4 cm^{-1} .

2.2.4. Thermal behaviour assessment

Thermogravimetric analysis was conducted on a TGA 2050 model from TA Instruments by heating samples contained in alumina pans at 10°C min⁻¹ from 40 °C to 700°C under nitrogen flow.

2.2.5. CHNS analysis investigations

To determine the elements in nanosponge and beta-cyclodextrin, CHNS analysis was conducted using a CHNS-O Analyser (FLASHEA 1112 series).

2.2.6. Particle size assessment by dynamic light scattering (DLS)

Determination of particle size of NS and CRC-NS was performed with a 90 plus particle sizer instrument (DLS) (Malvern, UK). The samples (100 mg) were diluted in distilled ethanol (10 ml) prior to measurements. The mean hydrodynamic diameter and polydispersity index of the particles were calculated at 25 °C with a scattering angle of 90°C.

2.2.7. Fourier transformed infra-red spectroscopy (FT-IR) investigations

Curcumin, nanosponge, complex and physical mixture were analysed by Fourier transform infra-red (FTIR) spectroscopy using JASCO 6300, Japan system 2000 FTIR Spectrophotometer in the region of 4000 cm⁻¹ – 400 cm⁻¹ and potassium bromide disc method.

2.2.8. X- ray powder diffraction investigations

Plain NS, curcumin, physical mixture and CRC-NS complex were subjected to XRD studies using X-ray powder diffraction (D8ADVANCE, Bruker, Germany). The radiation was Cobalt filtered Fe with a wavelength of 1.7890°A.

2.2.9. Differential scanning calorimetry (DSC) analysis investigations

Plain NS, curcumin, physical mixture and CRC-NS complex were subjected to scanning calorimeter. Samples were scanned at the rate of 10°C min−1 under nitrogen atmosphere in the temperature range of 30–250 °C.

2.2.10. Scanning electron microscopy (SEM) investigations

SEM was carried out by Field Emission Scanning Electron Microscopy (FESEM) (MIRA3 TESCAN, Czech Republic) with different magnifications for investigating the morphology of nanoparticles.

2.3. Encapsulation efficiency measurement

The predetermined weight of the complex was dissolved in 10 ml of methanol and then sonicated for 20 min (Kashi et al. 2012, Sareen et al. 2014). It was then centrifuged for 15 min at 25°C. The supernatant was

isolated and the drug content was analysed by UV Spectrophotometer (Biochrom biowave, UK) at 430 nm. Encapsulation efficiency of drug was calculated using Equation (1):

$$\%Drug\ encapsulation\ efficiency = \frac{Drug_{encapsulated}}{Drug_{total}} * 100 \qquad (1)$$

2.4. In vitro release of curcumin from nanosponge

In vitro release of curcumin from inclusion complex was investigated by membrane dialysis method against phosphate buffer (pH 7.4) at 37°C (Shende and Gaud 2009). Briefly, 150 μg of curcumin formulation was suspended in 3 ml of phosphate buffer (pH 7.4) and sonicated for 4 min. Then, it was placed in the dialysis tube (Sartorius, cut off 12,000 Da). At various time intervals, the content of phosphate buffer saline was centrifuged for 20 min at 10°C. Then, samples were withdrawn and analysed by UV spectrophotometer (Perkin Elmer) at 430 nm.

2.5. MTT assay investigations

The cytotoxicity of plain NS, curcumin and CRC-NS on L929 and MCF7 cell lines were investigated using MTT assay. Initially, cells were grown in Dulbecco's Modified Eagle's Medium (DMEM) as culture medium with 10% w/w Foetal Bovin Serum (FBS) and the combination of penicillin and streptomycin antibiotics (1% w/w). Storage conditions were 37°C incubated at 5 mbar with CO2 atmosphere. Cells in a certain number (8,000 cells per well) were cultured in a 96-well plate. The cells were then incubated for 24 and 48 h and were washed by PBS and evaluated by standard solution of MTT. After washing with PBS, 100 ml of a fresh intermediate was added to each well. Next, 10 μl of MTT solution was added to the cells and were placed in the incubator for 4 h. Then, the supernatant was evacuated of the wells and 100 μl of DMSO was added to each well and incubated in dark for 1 h. Finally, the optical absorbance of the solution was read on microplate Elisa reader (Bio-Rad, USA).

2.6. Haemolysis study investigations

In order to carry out this experiment, the blood containing EDTA was centrifuged at 1500 rpm for 5 min. The supernatant was removed and the precipitate was washed 3 times with phosphate buffer saline (PBS). Then, 200 μl of blood sediment was mixed with 3.8 ml of PBS and a few minutes of vortex. Samples were kept at room temperature for 2 h and then centrifuged for 5 min at about 1600 rpm. The supernatant absorbance was read at 541 nm. In this experiment, water was considered as a positive control and the PBS was considered as a negative control. After incubation, an optical microscope was used to see any malformation in blood cells. The percentage of haemolysis was calculated using Equation (2) (Assadi et al. 2018).

$$\%Haemolysis = \frac{ABS-ABS0}{ABS100-ABS0} * 100\% \qquad (2)$$

3. Results and discussion

3.1. NS characterisation

3.1.1. ATR-FTIR analysis results

The formation of the PMDA-β-CD nanosponge was confirmed by IR Spectroscopy by comparing the spectrum of the nanosponge with the spectrum of the individual β-CD (Figure 1a). There were significant peaks in

positions 1720 and 1580 cm^{-1} in nanosponge spectrum which belong to carboxyl and ester functional groups and carboxylate group of PMDA, respectively (Trotta et al. 2014). Therefore, it can be concluded that there was chemical interaction between the β-CD and PMDA. It should be mentioned that after several steps of washing with Ethanol and several days of purifying-washing cycles with acetone, the probability of free PMDA presence in the final compound is rare. Moreover, the intense characteristic peaks of PMDA which are observed in the nanosponge spectrum, indicates a significant interaction of β-CD and PMDA in the structure of nanosponge.
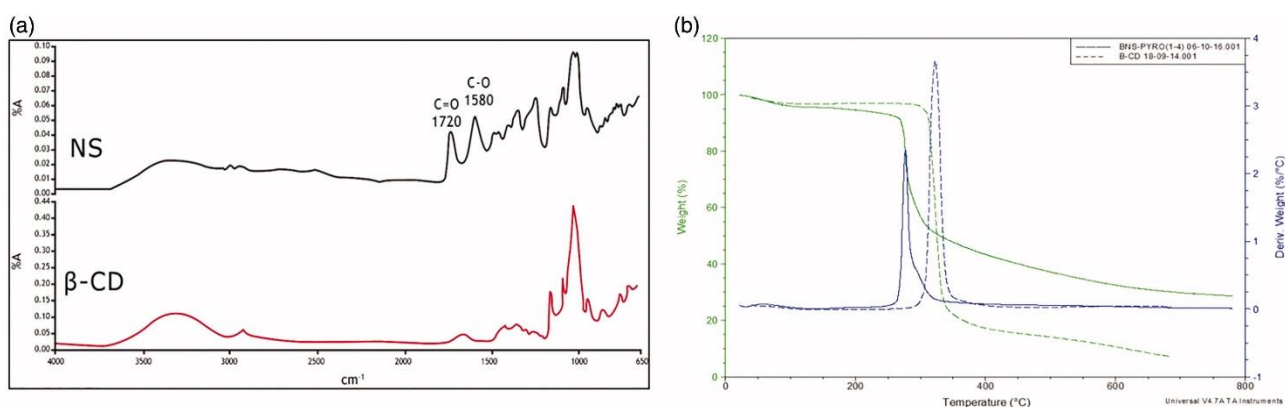

Figure 1. Confirmation of pyromellitic dianhydride-β-CD nanosponge formation by (a) Attenuated total reflectance- Fourier-transform infra-red spectroscopy (ATR-FTIR) spectrum of nanosponge and β-CD, (b) Thermogravimetric analysis (TGA) spectrum of nanosponge and β-CD.

3.1.2. TGA analysis results

In TGA curve of nanosponge, weight loss percentage is started in lower temperature comparing to the pure β-CD (Figure 1b). This phenomenon revealed that there exist weaker bonds in structure of nanosponge in comparison with pure β-CD which could be attributed to the nanosponge formation circumstances.

3.1.3. CHNS analysis results

CHNS analysis demonstrated different elements percentages before and after making nanosponges. The amount of N, C, H, and S were 0.00, 38.96, 6.58, and 0.00% for β-CD, and 3.39, 47.20, 6.30, and 0.00% for NS-PMDA(1:4). The negligible amount of nitrogen is due to the presence of a little amount of triethyl amine in nanosponge. Based on these results, changes occurred in the amount of C and H atoms are attributed to the fabrication of nanosponge from the β-CD.

3.2. CRC-NS characterisation results

3.2.1. Particle size analysis results

The particle size analysis of NS and CRC-NS suspensions demonstrated the 70 nm size of NS and CRC-NS with low polydispersity index (PDI = 0.42 ± 0.04). The particle size distribution is uniform with a narrow range (data not shown here).

3.2.2. FTIR analysis results

The comparison of FTIR spectra of curcumin, NS, their physical mixture and their complex is shown in Figure 2. There are two main characteristics peaks of plain nanosponge around 1720 cm^{-1}~1750 cm^{-1} and 1590 cm^{-1} attributed carboxyl group (C=O) justifying the formation of nanosponges from β-CD (Trotta et al. 2014). Moreover, there were other characteristics peaks of NS at 1030 cm^{-1}, 1451 cm^{-1} that are respectively attributed to C–O stretching vibration of primary alcohol and C-H bending vibration of alkane. The spectrum curcumin demonstrated its dominant characteristic peaks at 1027 cm^{-1} (C–O–C stretching vibrations), 1277 cm^{-1} (aromatic C–O stretching vibration), 1428 cm^{-1} (olefinic C–H bending vibration), 1509 cm^{-1} (C=C and C=O vibrations), 1623 cm^{-1} (C=C stretching vibrations of benzene ring) and a peak at 3508 cm^{-1} (phenolic O-H). In physical mixture, the main peaks of pure curcumin (1027, 1277, 1428, 1509, 1623 and 3508) and plain nanosponge (1720–1750, 1590) present simultaneously, which indicates that there is no chemical reaction between two components. By formation of inclusion complex between curcumin and the nanosponge, all main peaks of nanosponge were emerged, whereas that of curcumin disappeared.
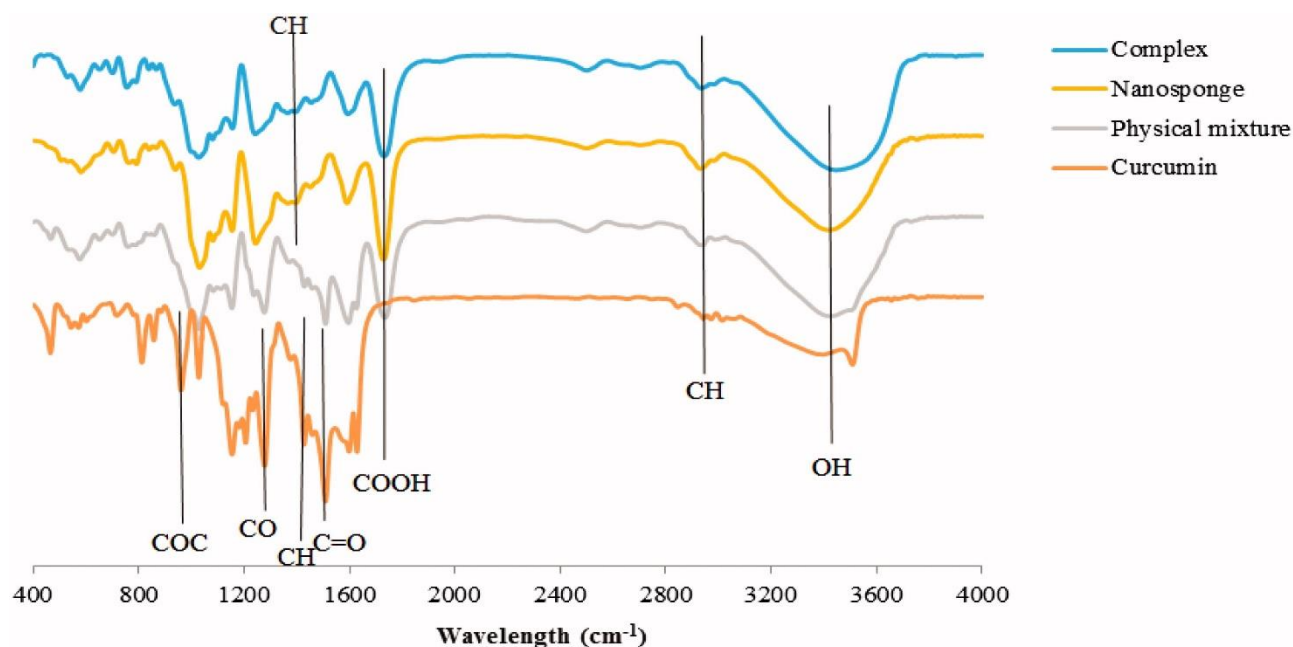

Figure 2. Fourier-transform infra-red spectroscopy spectra of curcumin, physical mixture, nanosponge and curcumin-nanosponge complex confirming the formation of pyromellitic dianhydride-β-CD nanosponge.

3.2.3. XRD analysis results

In order to investigate the crystalline features of the compounds, the XRD patterns of pure nanosponge, curcumin, physical mixture and CRC-NS were assessed. Curcumin has a crystalline structure. It is shown in Figure 3 that pure curcumin has distinct peaks (with two manifest peaks) indicating its crystalline structure, whereas that of nanosponge, did not show any definite peak, suggesting that the nanosponge has no crystalline structure. In the physical mixture of these two components, the trend is a combination of two previous diagrams, indicating a poor mechanical interaction between these two compounds. It is evidently shown that the main curcumin peaks have completely been disappeared and a new trend emerges, indicating that the drug presents in the nanosponge cavities.
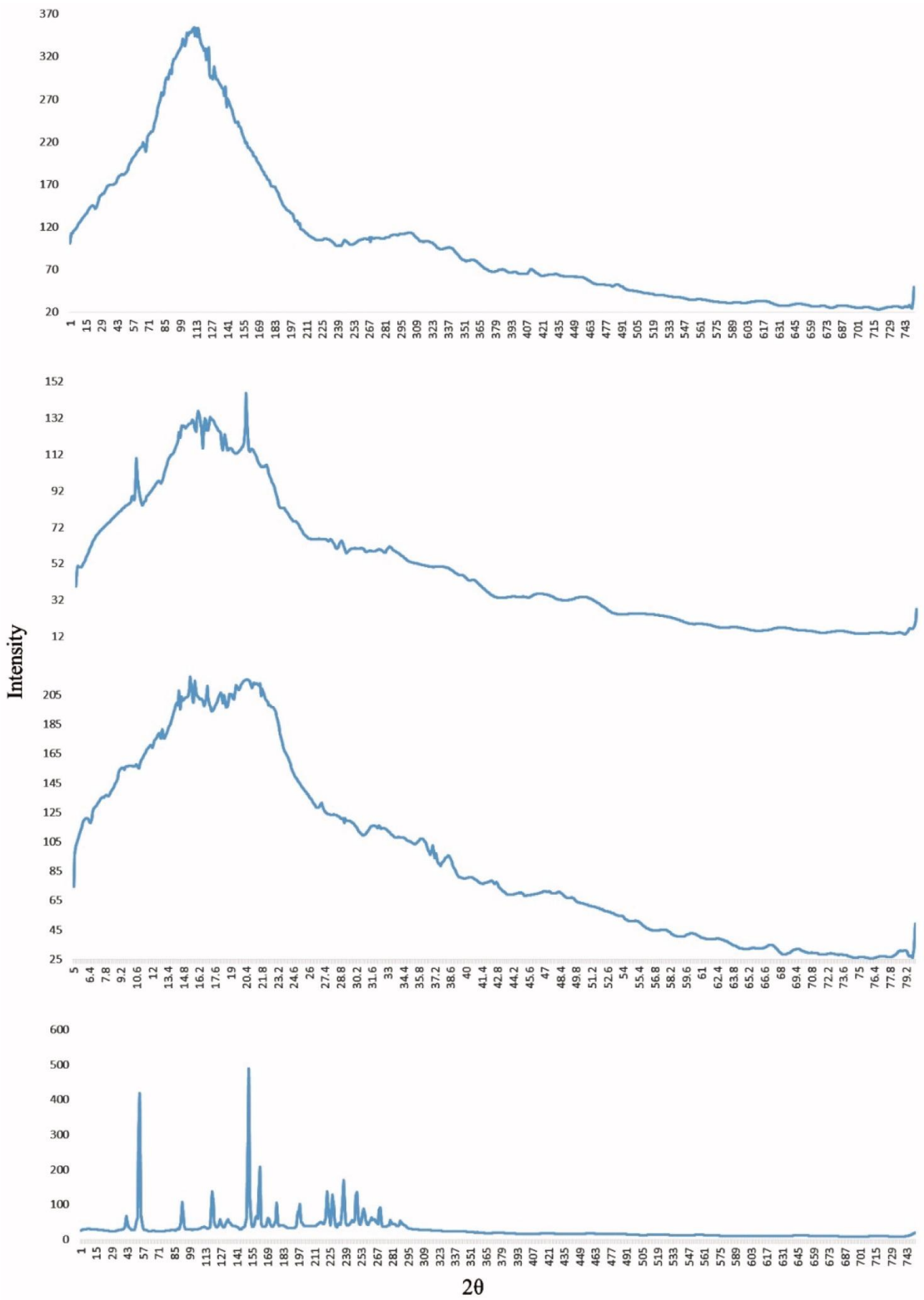
Figure 3. XRD pattern of (a) curcumin-nanosponge complex, (b) physical mixture, (c) nanosponge and d) curcumin confirming the formation of pyromellitic dianhydride-β-CD nanosponge.

3.2.4. DSC analysis results

DSC curves of pure curcumin, nanosponge, their physical mixture, and their complex are shown in Figure 4. The thermal behaviour of curcumin demonstrated a sharp peak around 178°C, which is attributed to the curcumin melting point. For NS, there is a broad peak at 124°C, which is due to the outflow of water molecules from the nanosponge cavities, and the main endothermic peak is located at 350°C. In the physical mixture, as evidenced in Figure 4, both peaks of curcumin (178°C) and NS (124°C) are present because both of these compounds separately exist without chemical interactions. In the complex curve, the endothermic peak of curcumin has been disappeared, indicating that curcumin is enclosed within the nanosponge cavities. Therefore, by encapsulating, the drug is protected and its stability is increased. (Anandam and Selvamuthukumar 2014, Singireddy and Subramanian 2016).
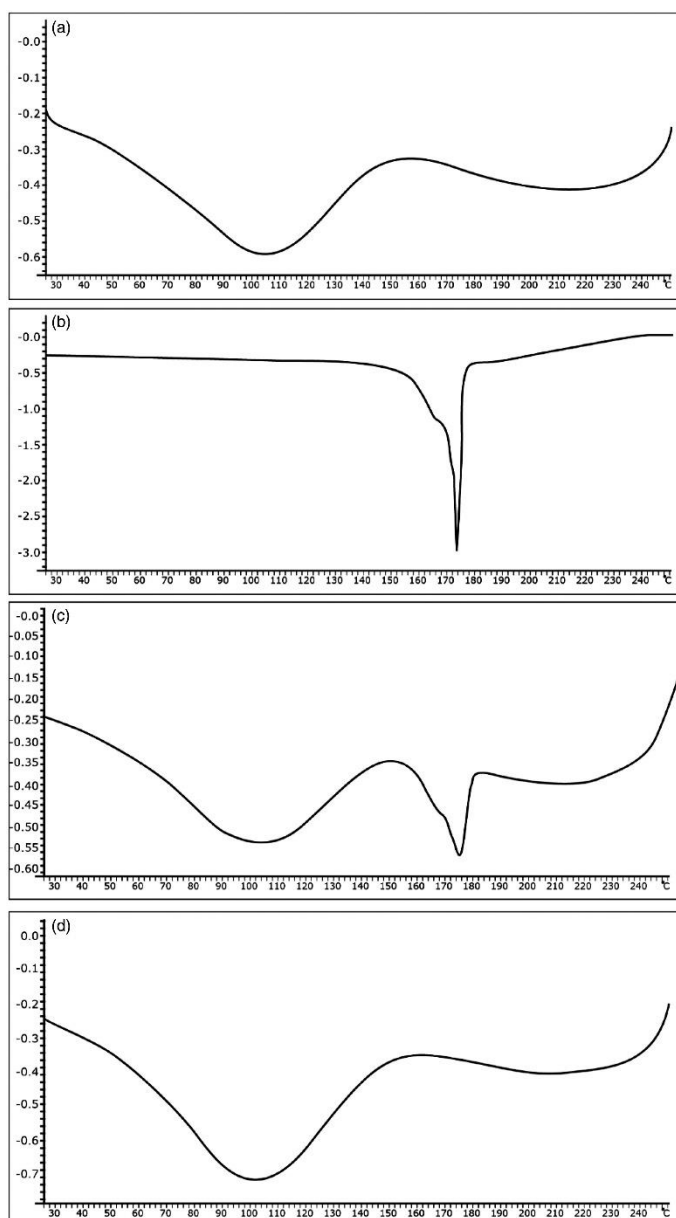
Figure 4. DSC thermogram of (a) nanosponge, (b) curcumin, (c) physical mixture, (d) curcumin-nanosponge complex confirming the formation of pyromellitic dianhydride-β-CD nanosponge.

3.2.5. SEM morphology assessment results

To investigate the morphology and apparent properties of nanosponge, curcumin, their physical mixture and their complex, scanning electron microscopy (SEM) was used and the results are shown in Figure 5. According to the SEM images curcumin has a crystalline structure. The electron microscopy images of the nanosponge show a spherical and porous structure for this material. In the physical mixture, the presence of curcumin with a crystalline structure and nanosponge with an amorphous structure could be seen evidently, which confirms that no chemical or physical interaction has taken place between the two substances. In the images of the complex, the porous nanoparticle structure is quite evident after encapsulation and the curcumin crystalline state is not visible due to its placement in the nanosponge cavities and the formation of an inclusion complex.
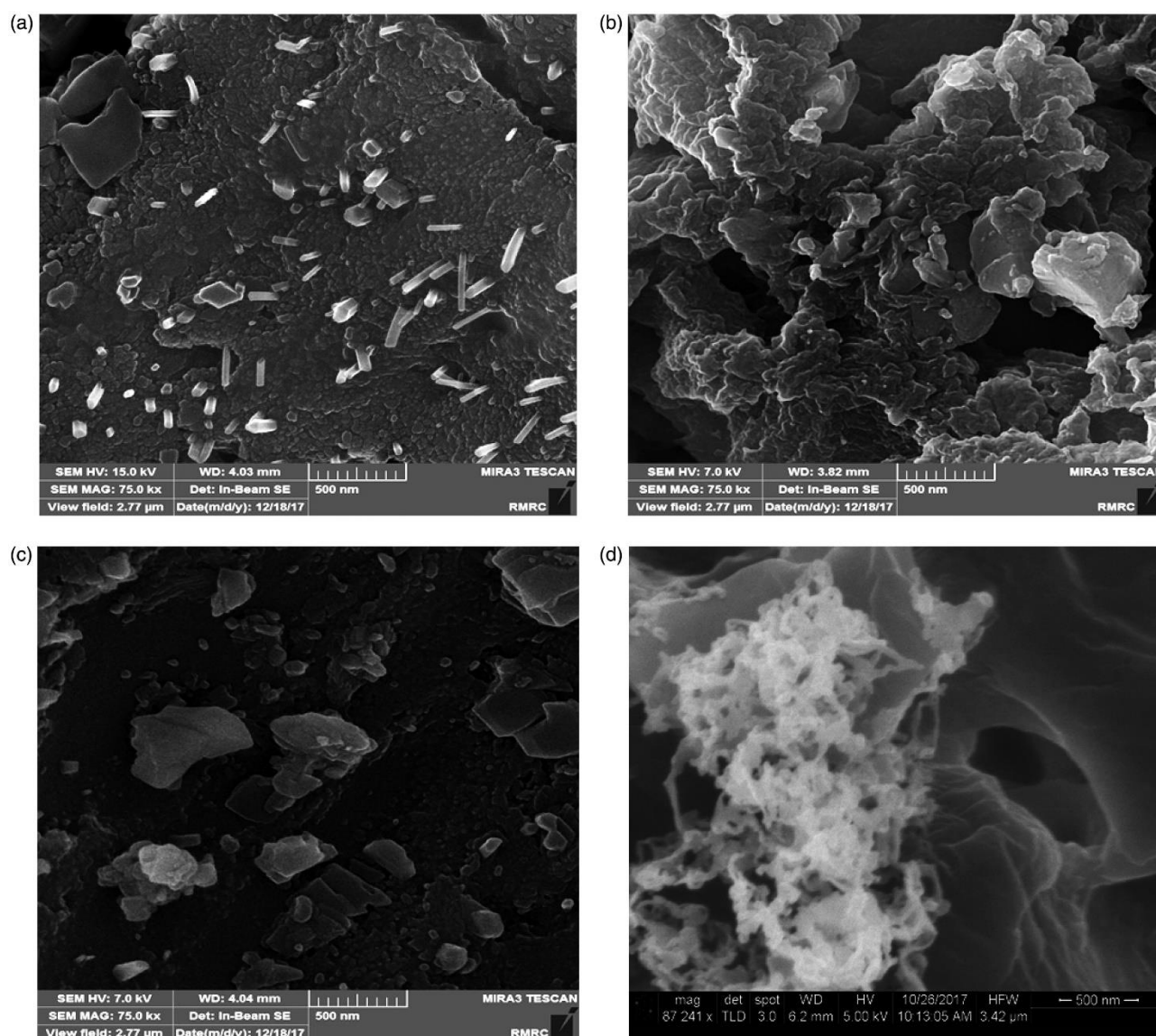
Figure 5. Scanning Electron Microscopy results of (a) curcumin, (b) nanosponge, (c) physical mixture and (d) curcumin-nanosponge complex confirming the formation of pyromellitic dianhydride-β-CD nanosponge.

3.3. Encapsulation efficiency; effect of drug initial concentrations and time

The encapsulation efficiency of curcumin with different drug concentrations was investigated, and the results showed that the drug initial concentration did not have significant effect on the encapsulation efficiency. It was 98.66, 98.16, and 98.12% w/w for curcumin concentrations of 17.89, 4.41, and 2.57 mg/ml, respectively.

The amount of encapsulation of curcumin was also investigated over three time periods. The results showed no significant difference over 24, 48 and 72 h, in which the drug encapsulation amount was 98.16, 98.27, and 98.35% w/w, respectively. Therefore, the time interval of 24 was selected for drug loading.

3.4. Drug release investigations

As it is clear from the release pattern (Figure 6a), the release of curcumin from the nanosponge takes place in two steps. In the first 8 h, its release is rather rapid. The release at this time period is related to the part of the curcumin molecules that are located at the surface of the nanosponge matrix, so they are released in the first hours. The second part of the release occurs after 8 h at a moderate and slow speed and is related to release of drug molecules that are spread within the complex and have more strong connection to the nanosponge than the surface molecules.
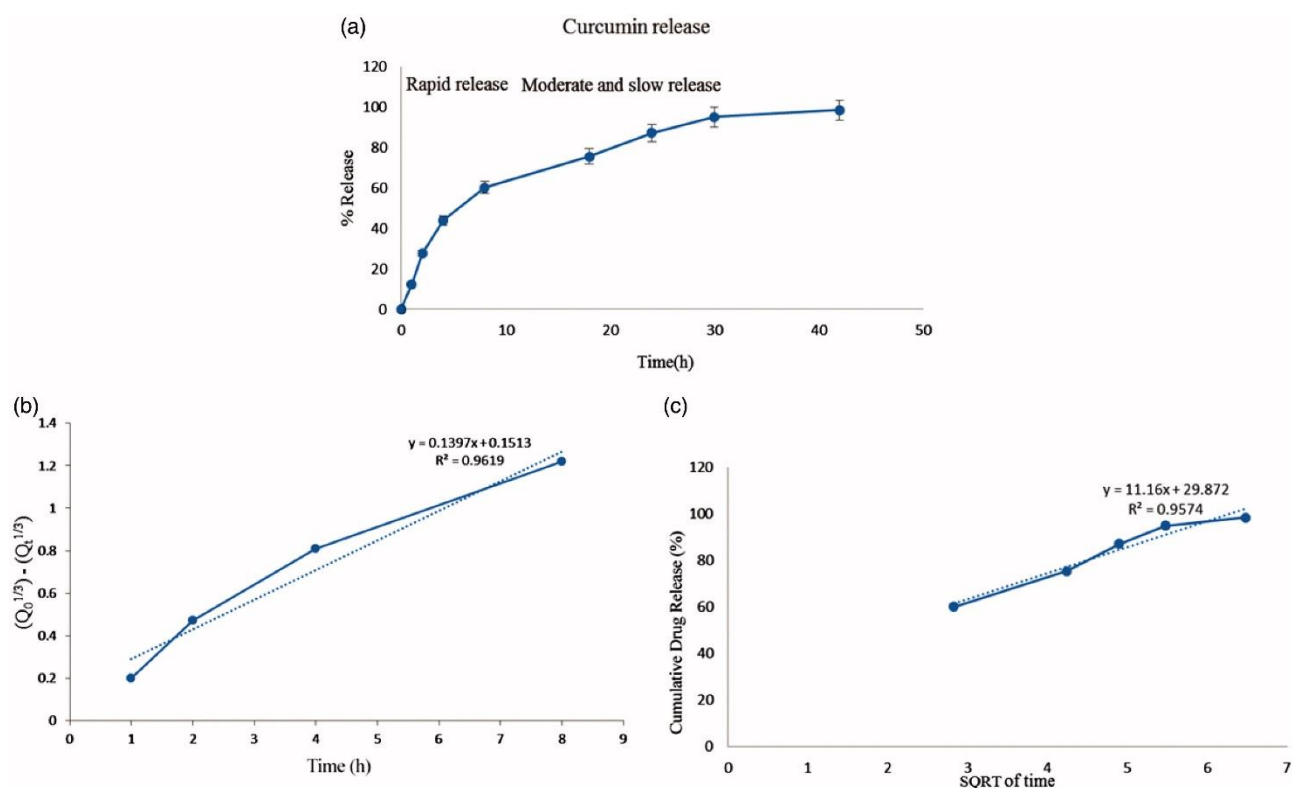

Figure 6. (a) In vitro release of curcumin from nanosponge (n = 3), which shows three distinct rapid, moderate, and slow release of drug, and the release kinetic results for (b) Hixson-Crowell and (c) Higuchi models. Hixson-Crowell model: $Q_0^{1/3} - Q_t^{1/3} = K_S t$, and Higuchi model: $Q/Q_0 = K_H \times t^{1/2}$, where Q_0 is initial drug

value, Q_t is the amount of drug released at time t, K_S is a constant incorporating the surface volume relation, K_H is the Higuchi dissolution constant.

Releasing rate is calculated 87% w/w in 24 h and 98% w/w in total. The controlled release of curcumin suggests that it is encapsulated in the nanosponge through forming an inclusion complex. Controlled release of curcumin reduces its toxic effects with fewer side effects. Releasing of curcumin follows two kinetic models. Since the substrate used for drug loading in this study has a porous structure with cyclodextrins both in the surface and within the cavities, the drug is linked both to the surface of the cyclodextrin and in the cavities. The release of drugs attached to the surface of nanostructure is more rapid due to the lack of spatial inhibition, which is evident in its release pattern that shows a fast release within the first 8 h. This type of release follows well the Hixson-Crowell release kinetic model (Figure 6b). On the other hand, drugs that are located inside the nanosponge cavities have a slower release and are released according to the penetration effect (Fickian diffusion). This is clearly evident in its release graph and can be verified according to the Higuchi release kinetic model (Figure 6c) (Barzegar-Jalali et al. 2008, Chime et al. 2013, Kayani et al. 2018).

3.5. Cytotoxicity investigations

The results of the effect of pure nanosponge, curcumin and the complex on human breast cancer cells (MCF7) and healthy cells (L929) has been shown in Figure 7. These results are attributed to the effect of different concentrations of samples (4 different concentrations of the complex, three concentrations of curcumin and one concentration of nanosponge) on the survival of cells in 24 and 48 h. According to the results, nanosponge does not have toxic effects on healthy cells and has a little toxicity on cancerous cells during the first 24 h, with no toxicity over the next 48 h while the drug is toxic to healthy and cancerous cells, it is more toxic to cancer cells than healthy cells. Nevertheless, all complex concentrations are shown to be safe for healthy cells, and significantly toxic to cancer cells.
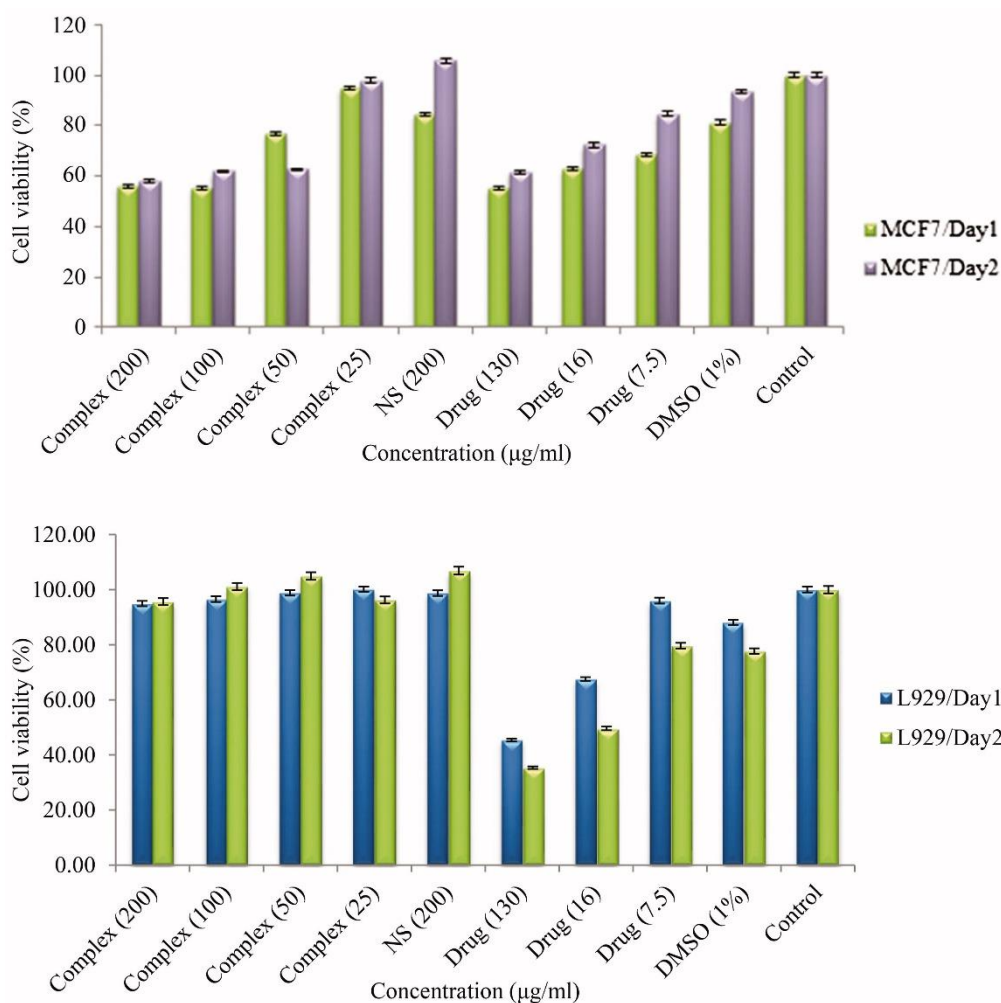
Figure 7. The cytotoxicity investigations results using MTT assay on (A) human breast cancer cells (MCF7), and (B) healthy cells (L929) (n = 3).

3.6. Haemolysis investigations

According to previous studies, nanosponge suspension in water, even at high concentrations of 20 mg ml^{-1} does not have haemolytic effects on blood cells (Darandale and Vavia 2013). In this study, haemolysis test was used to assess the blood compatibility of nanosponge. According to the experiments, the nanosponge did not cause haemolysis at moderate concentration (50 and 100 mg ml^{-1}) with negligible haemolysis at high concentrations of 200 mg ml^{-1} (Figure 8). Blood cells also exhibited considerable tolerance to the complex. Studies have shown that after incubation with nanosponge, almost 99.5% of the blood cells were survived. The optical microscopy assessment of cells determined that these cells are remained unscathed after the incubation with nanosponge, which confirms its blood compatibility.
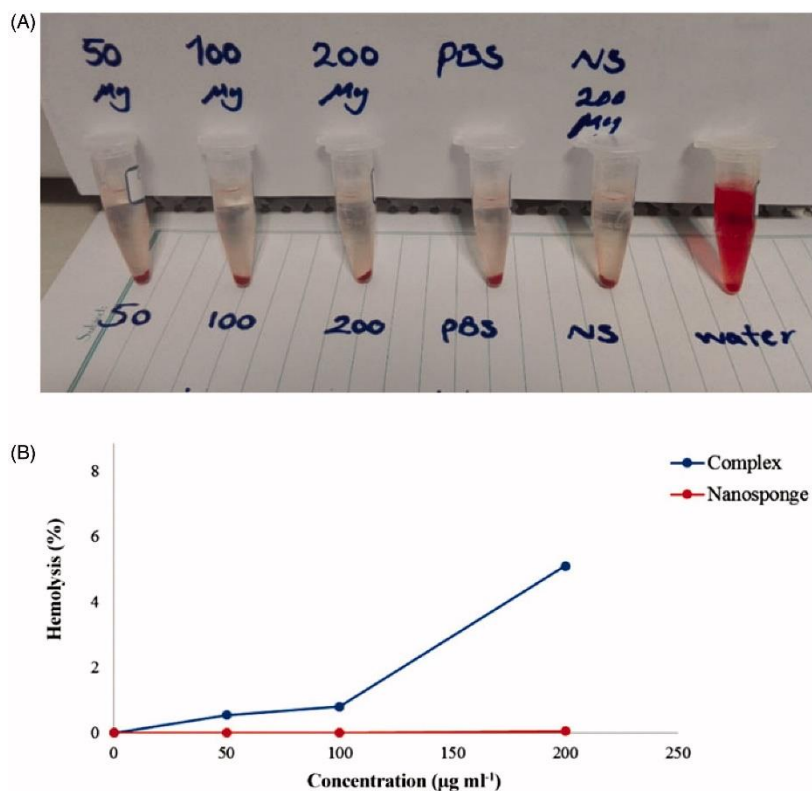
Figure 8. The (A) visual, and (B) diagram results of haemolysis study of 50, 100 and 200 µg curcumin-nanosponge complex, PBS, nanosponge and water, demonstrating no haemolysis for nanosponge at moderate concentration (50 and 100 mg ml^{-1}) and negligible haemolysis at high concentrations.

4. Conclusions

The purpose of this study was to synthesise a drug delivery nanosystem capable of encapsulating the drug, increasing its sustainability and inducing controlled release. The results of various characterisation techniques justified nanosponge synthesis and drug loading by this nanosystem. Increased drug stability was confirmed by DSC. The drug release assessment showed a sustained release in 42 h. The results of this study showed that nanosponge is biocompatible and non-haemolytic, and as a drug delivery system, it has improved the drug properties and thus could be widely considered in cancer treatment.

Disclosure statement

No potential conflict of interest was reported by the authors.

References

Aggarwal, B.B., Kumar, A., and Bharti, A.C., 2003. Anticancer potential of curcumin: preclinical and clinical studies. Anticancer research, 23(1A), 363–398.

Allahyari, S., et al., 2019. Cyclodextrin-based nanosponges as promising carriers for active agents. Expert opinion on drug delivery, 16(5), 467–479.

Amanlou, N., et al., 2019. Enhanced cytotoxic activity of curcumin on cancer cell lines by incorporating into gold/chitosan nanogels. Materials chemistry and physics, 226, 151–157.

Anand, P., et al., 2007. Bioavailability of curcumin: problems and promises. Molecular pharmaceutics, 4(6), 807–818.

Anandam, S., and Selvamuthukumar, S., 2014. Fabrication of cyclodextrin nanosponges for quercetin delivery: physicochemical characterization, photostability, and antioxidant effects. Journal of materials science, 49(23), 8140–8153.

Ansari, K.A., et al., 2011. Cyclodextrin-based nanosponges for delivery of resveratrol: in vitro characterisation, stability, cytotoxicity and permeation study. Aaps pharmscitech, 12(1), 279–286.

Assadi, Z., Emtiazi, G., and Zarrabi, A., 2018. Novel synergistic activities of tetracycline copper oxide nanoparticles integrated into chitosan micro particles for delivery against multiple drug resistant strains: generation of reactive oxygen species (ROS) and cell death. Journal of drug delivery science and technology, 44, 65–70.

Barzegar-Jalali, M., et al., 2008. Kinetic analysis of drug release from nanoparticles. Journal of pharmacy and pharmaceutical sciences, 11(1), 167–177.

Baum, L., et al., 2008. Six-month randomized, placebo-controlled, double-blind, pilot clinical trial of curcumin in patients with Alzheimer disease. Journal of clinical psychopharmacology, 28(1), 110–113.

Bhatia, S., 2016. Nanoparticles types, classification, characterization, fabrication methods and drug delivery applications. In: Bhatia S. eds. Natural polymer drug delivery systems. Switzerland: Springer, 33–93.

Bose, R.J., Lee, S.-H., and Park, H., 2016. Biofunctionalized nanoparticles: an emerging drug delivery platform for various disease treatments. Drug discovery today, 21(8), 1303–1312.

Boyanapalli, S.S., and Kong, A.-N.T., 2015. Curcumin, the king of spices: epigenetic regulatory mechanisms in the prevention of cancer, neurological, and inflammatory diseases. Current pharmacology reports, 1(2), 129–139.

Campos, C.A., et al., 2013. Design, synthesis, and evaluation of curcumin-derived arylheptanoids for glioblastoma and neuroblastoma cytotoxicity. Bioorganic & medicinal chemistry letters, 23, 6874–6878.

Chime, S., Onunkwo, G., and Onyishi, I., 2013. Kinetics and mechanisms of drug release from swellable and non swellable matrices: a review. Research journal of pharmaceutical, biological and chemical sciences, 4, 97–103.

Darandale, S., and Vavia, P., 2013. Cyclodextrin-based nanosponges of curcumin: formulation and physicochemical characterization. Journal of inclusion phenomena and macrocyclic chemistry, 75(3-4), 315–322.

Deshmukh, K., and Shende, P., 2018. Toluene diisocyanate cross-linked β-cyclodextrin nanosponges as a pH-sensitive carrier for naproxen. Materials research express, 5(7), 075008.

Ferro, M., et al., 2014. Anomalous diffusion of Ibuprofen in cyclodextrin nanosponge hydrogels: an HRMAS NMR study. Beilstein journal of organic chemistry, 10, 2715–2723.

Gupta, S.C., Kismali, G., and Aggarwal, B.B., 2013. Curcumin, a component of turmeric: from farm to pharmacy. Biofactors, 39(1), 2–13.

Hamzehzadeh, L., et al., 2018. The versatile role of curcumin in cancer prevention and treatment: a focus on PI3K/AKT pathway. Journal of cellular physiology, 233(10), 6530–6537.

Hewlings, S.J., and Kalman, D.S., 2017. Curcumin: a review of its' effects on human health. Foods, 6(10), 92.

Imanifard, S., et al., 2017. Nanoengineered Thermoresponsive Magnetic Nanoparticles for Drug Controlled Release. Macromolecular chemistry and physics, 218(23), 1700350.

Islami, M., et al., 2018. Controlled quercetin release from high-capacity-loading hyperbranched polyglycerol-functionalized graphene oxide. International journal of nanomedicine, 13, 6059.

Jahed, V., et al., 2014. NMR (1H, ROESY) spectroscopic and molecular modelling investigations of supramolecular complex of β-cyclodextrin and curcumin. Food chemistry, 165, 241–246.

Kashi, T.S.J., et al., 2012. Improved drug loading and antibacterial activity of minocycline-loaded PLGA nanoparticles prepared by solid/oil/water ion pairing method. International journal of nanomedicine, 7, 221–234.

Kayani, Z., Firuzi, O., and Bordbar, A.-K., 2018. Doughnut-shaped bovine serum albumin nanoparticles loaded with doxorubicin for overcoming multidrug-resistant in cancer cells. International journal of biological macromolecules, 107, 1835–1843.

Khorrami, S., et al., 2018. Selective cytotoxicity of green synthesized silver nanoparticles against the MCF-7 tumor cell line and their enhanced antioxidant and antimicrobial properties. International journal of nanomedicine, 13, 8013.

Kurkov, S.V., and Loftsson, T., 2013. Cyclodextrins. International journal of pharmaceutics, 453(1), 167–180.

Lao, C.D., et al., 2006. Dose escalation of a curcuminoid formulation. BMC complementary and alternative medicine, 6(1), 10.

Lembo, D., Trotta, F., and Cavalli, R., 2018. Cyclodextrin-based nanosponges as vehicles for antiviral drugs: challenges and perspectives. Nanomedicine, 13(5), 477–480.

Maheshwari, R.K., et al., 2006. Multiple biological activities of curcumin: a short review. Life sciences, 78(18), 2081–2087.

Mousavi, H., et al., 2015. A multifunctional hierarchically assembled magnetic nanostructure towards cancer nano-theranostics. RSC advances, 5(94), 77255–77263.

Moya-Ortega, M.D., et al., 2012. Cyclodextrin-based nanogels for pharmaceutical and biomedical applications. International journal of pharmaceutics, 428(1-2), 152–163.

Nelson, K.M., et al., 2017. The essential medicinal chemistry of curcumin: miniperspective. Journal of medicinal chemistry, 60(5), 1620–1637.

Pochampally, R., et al., 2017. Curcumin-loaded γ-cyclodextrin liposomal nanoparticles as delivery vehicles for osteosarcoma. Nanomedicine in cancer, 8(4), 440–452.

Pushpalatha, R., Selvamuthukumar, S., and Kilimozhi, D., 2018. Cross-linked, cyclodextrin-based nanosponges for curcumin delivery-physicochemical characterization, drug release, stability and cytotoxicity. Journal of drug delivery science and technology, 45, 45–53.

Rao, T.S., Basu, N., and Siddiqui, H., 2013. Anti-inflammatory activity of curcumin analogues. Indian journal of medical research, 137, 841–845.

Rauf, A., et al., 2018. Health perspectives of a bioactive compound curcumin: a review. Trends in food science & technology, 74, 33–45.

Ravindran, J., Prasad, S., and Aggarwal, B.B., 2009. Curcumin and cancer cells: how many ways can curry kill tumor cells selectively? The AAPS journal, 11(3), 495–510.

Rezaei, A., et al., 2019. Improving the solubility and in vitro cytotoxicity (anticancer activity) of ferulic acid by loading it into cyclodextrin nanosponges. International journal of nanomedicine, 14, 4589.

Saokham, P., et al., 2018. Solubility of cyclodextrins and drug/cyclodextrin complexes. Molecules, 23(5), 1161–1176.

Sareen, R., et al., 2014. Curcumin loaded microsponges for colon targeting in inflammatory bowel disease: fabrication, optimization, and in vitro and pharmacodynamic evaluation. BioMed research international, 2014, 1.

Shende, P., and Gaud, R., 2009. Formulation and comparative characterization of chitosan, gelatin, and chitosan–gelatin-Coated Liposomes of CPT-11–HCl. Drug development and industrial pharmacy, 35(5), 612–618.

Shende, P., et al., 2015. Acute and repeated dose toxicity studies of different β-cyclodextrin-based nanosponge formulations. Journal of pharmaceutical sciences, 104(5), 1856–1863.

Sherje, A.P., et al., 2017. Cyclodextrin-based nanosponges: a critical review. Carbohydrate polymers, 173, 37–49.

Simionato, I., et al., 2019. Encapsulation of cinnamon oil in cyclodextrin nanosponges and their potential use for antimicrobial food packaging. Food and chemical toxicology, 132, 110647.

Singireddy, A., and Subramanian, S., 2016. Cyclodextrin nanosponges to enhance the dissolution profile of quercetin by inclusion complex formation. Particulate science and technology, 34(3), 341–346.

Tejashri, G., Amrita, B., and Darshana, J., 2013. Cyclodextrin based nanosponges for pharmaceutical use: A review. Acta pharmaceutica, 63(3), 335–358.

Trotta, F., and Mele, A., 2019. Nanosponges: Synthesis and Applications. Weinheim, Germany: Wiley-VCH.

Trotta, F., 2011. Cyclodextrin nanosponges and their applications. In: E. Bilensoy, ed. Cyclodextrins in pharmaceutics, cosmetics, and biomedicine: Current and future industrial applications, Hoboken, NJ: John Wiley & Sons, 323–342.

Trotta, F., et al., 2014. Synthesis and characterization of a hyper-branched water-soluble β-cyclodextrin polymer. Beilstein journal of organic chemistry, 10, 2586.

Trotta, F., Tumiatti, W. & Vallero, R. 2004. Nanospugne a base di ciclodestrine funzionalizzate con gruppi carbossilici: sintesi e utilizzo nella decontaminazione da metalli pesanti e da composti organici. Italian Patent No. MI2004A000614. 2004-03-30.

Trotta, F., Zanetti, M., and Cavalli, R., 2012. Cyclodextrin-based nanosponges as drug carriers. Beilstein journal of organic chemistry, 8, 2091–2099.

Vallianou, N.G., et al., 2015. Potential anticancer properties and mechanisms of action of curcumin. Anticancer research, 35(2), 645–651.

Vishwakarma, A., et al., 2014. Review on nanosponges: a benefication for novel drug delivery. International journal of PharmTech research, 6, 11–20.

Wang, Y., et al., 2018. Nanomaterials for cancer precision medicine. Advanced materials, 30(17), 1705660.

Wright, J.S., 2002. Predicting the antioxidant activity of curcumin and curcuminoids. Journal of molecular structure: theochem, 591(1–3), 207–217.

Zarrabi, A., et al., 2011. Design and synthesis of novel polyglycerol hybrid nanomaterials for potential applications in drug delivery systems. Macromolecular bioscience, 11(3), 383–390.

Zarrabi, A., et al., 2014. In vitro biocompatibility evaluations of hyperbranched polyglycerol hybrid nanostructure as a candidate for nanomedicine applications. Journal of materials science: materials in medicine, 25, 499–506.